1995ApJ...451..436C

THE ASTROPHYSICAL JOURNAL, 451:436–443, 1995 October 1
© 1995. The American Astronomical Society. All rights reserved. Printed in U.S.A.

BACKGROUND X-RAY EMISSION FROM HOT GAS IN CDM AND CDM+Λ UNIVERSES: SPECTRAL SIGNATURES

RENYUE CEN,[1] HYESUNG KANG,[1,2] JEREMIAH P. OSTRIKER,[1] AND DONGSU RYU[1,3]
Received 1995 January 30; accepted 1995 April 11

ABSTRACT

We present a new treatment of two popular models for the growth of structure, examining the X-ray emission from hot gas with allowance for spectral line emission from various atomic species, primarily "metals." The X-ray emission from bright cluster sources is not significantly different from that found in prior work and, as noted earlier, shows that the CDM+Λ model is consistent but the standard, *COBE*-normalized model is inconsistent with existing observations—after allowance for the still considerable numerical modeling uncertainties.

But we find one important new result. Radiation in the softer band 0.5–1.0 keV is predominantly emitted by gas far from cluster centers (hence "background"). This background emission dominates the cluster emission below 1 keV, and observations of it should show clear spectral signatures indicating its origin. In particular, the "iron blend" should be seen prominently in this spectral bin from cosmic background hot gas at high galactic latitudes and should show shadowing against the SMC indicating its extragalactic origin. Certain O VII lines also provide a signature of this gas which emits a spectrum characteristic of $10^{6.6\pm0.6}$ K gas. Recent *Advanced Satellite for Cosmology and Astrophysics* observations of the X-ray background tentatively indicate the presence of components with exactly the spectral features we predict here.

Subject headings: cosmology: theory — dark matter — diffuse radiation — large-scale structure of universe — radiation mechanisms: nonthermal

1. INTRODUCTION

In three preceding papers, Kang et al. (1994), Bryan et al. (1994), Cen & Ostriker (1994), we investigated the X-ray cluster properties in the standard *COBE*-normalized cold dark matter (CDM) model and in a CDM model with a cosmological constant, under the assumption that bremsstrahlung was the primary emission process. While this assumption is an excellent approximation for hard X-ray bands ($h\nu > 2$ keV), which characterize the emission from the great clusters, its validity in softer bands has to be examined more carefully. In this paper, we include detailed X-ray line emissions from 12 major elements (He, C, N, O, Ne, Mg, Si, S, Ar, Ca, Fe, and Ni), in addition to bremsstrahlung due to these elements, and we shift focus to the lower luminosity, lower temperature clusters, filaments, and sheets that would normally be considered part of the "X-ray background." We compare the X-ray cluster luminosity functions and X-ray background radiation fields, with and without line emission at different bands, for both cosmological models. The issue of cooling flows in cluster centers is also addressed in an approximate fashion, and detailed X-ray spectra of a few bright X-ray clusters are presented. Finally, we compute the "background" emission from hot gas in the two models—the line and continuum emission from gas far from the centers of rich clusters. Our primary new result is that the extragalactic background radiation field due to hot gas far from the centers of rich clusters is surprisingly large and dominates other (diffuse) sources at energies below 1 keV.

Very recent observations (Gendreau et al. 1994) of the spectrum of the X-ray background clearly indicate a thermal component from evidence for O VII and O VIII lines. The data also show "an excess above the extrapolation of the single power-law model below 1 keV" of exactly the nature we describe in § 3.2.

In this paper we concentrate on the spectral signature of the background gas. A subsequent paper (Cen et al. 1995) will focus on the spatial distribution; we note here in anticipation of that paper that the angular autocorrelation function of the hot gas in our simulations does (due to the background gas component) show the extended features (up to several degrees) seen in the real data (Soltan et al. 1995).

The present paper is organized as follows: § 2 describes our method of including line emission processes, § 3 gives the results and comparisons with observations, and our conclusions are assembled in § 4.

2. METHOD

The cosmological models we investigate here are the same ones that we studied previously: (1) the standard, *COBE*-normalized CDM model (SCDM) with $\Omega = 1$, $H = 50$ km s^{-1} Mpc^{-1}, $\sigma_8 = 1.05$, and $\Omega_b = 0.06$ (Kang et al. 1994) and (2) a *COBE*-normalized, flat CDM model with a cosmological constant (LCDM) with $\Omega = 0.45$, $\lambda = 0.55$, $H = 60$ km s^{-1} Mpc^{-1}, $\sigma_8 = 0.77$, and $\Omega_b = 0.043$ (Cen & Ostriker 1994). Both model simulations are performed in a box of size 85 h^{-1} Mpc with 270^3 cells and 135^3 dark matter particles. These simulations were run in an adiabatic fashion, i.e., no cooling/heating processes were included except for shock heating, which is intrinsic to the simulations and hence automatically included. After the simulations were completed, we calculated line emission and continuum emission from heavy elements, in addition to those due to H and He, simply by assuming that the metals should be present in the cosmic gas, at the observed abundances. The excluded dynamic effect of cooling/heating due to the metals, which are not present in the original simula-

[1] Princeton University Observatory, Princeton, NJ 08544; cen@astro.princeton.edu.
[2] Department of Earth Sciences, Pusan National University, Pusan, Korea.
[3] Department of Astronomy and Space Science, Chungnam National University, Daejun, Korea.

© American Astronomical Society • Provided by the NASA Astrophysics Data System

1995ApJ...451..436C

tions, is probably unimportant because the cooling/heating time is typically much longer than the dynamical time of the systems under consideration, as we will show below.

The X-ray clusters in the simulations are identified in exactly the same way as before; see Kang et al. (1994) for details. The metallicity in different (density) regions is assumed to have the following form:

$$Z(\rho_{\rm sm}) = 0.35 \times [1 - e^{-(\rho_{\rm sm}/\bar{\rho}_b)^2}] , \quad (1)$$

where $Z(\rho_{\rm sm})$ is in units of solar metallicity, $\rho_{\rm sm}$ is the baryonic density of the region in question smoothed over a Gaussian window of radius 1 h^{-1} Mpc, and $\bar{\rho}_b$ is the global mean of the baryonic density. This approximate formula is not intended to be very accurate, but it suffices for our needs. Equation (1) will produce for high-density regions the metallicity observed in the great clusters, 0.35 (Edge & Stewart 1991; Arnaud et al. 1992, 1994). Then for regions with low density, $\rho_{\rm sm}$, the metallicity declines rapidly, giving for gas in the voids ($\rho_{\rm sm}/\bar{\rho}_b \approx 0.1$) a metallicity of 3.5×10^{-2} $Z_\odot$, consistent with estimates/bounds obtained from studies of QSO absorption lines (Fan & Tytler 1994; Cowie et al. 1995).

The X-ray emissivity is calculated with a code, kindly made available to us by J. C. Raymond, based on the work of Raymond & Smith (1977). It is assumed that the gas is in ionization equilibrium and optically thin. The photoionization by the diffuse radiation is ignored in the present study since collisional ionization dominates photoionization for $T \gg 10^5$ K. the solar abundances are taken from the CLOUDY code (Ferland 1994): C (8.56), N (8.05), O (8.93), Ne (8.09), Mg (7.58), Si (7.55), S (7.21), Ar (6.56), Ca (6.36), Fe (7.67), and Ni (6.25). The He abundance is assumed to be 10.90, consistent with standard light-element nucleosynthesis. The emission rates from H, He, and metals are calculated separately. Then each component is weighted by the relative abundance, and the sum of all components is our total emissivity. We use the following energy bins to generate the spectra: 0.5 eV for $h\nu$ = 1–100 eV, 5 eV for $h\nu$ = 100–1000 eV, 20 eV for $h\nu$ = 1–10 keV, 40 eV for $h\nu$ = 10–50 keV, and 100 eV for $h\nu$ = 50–1000 keV.

3. RESULTS AND COMPARISONS WITH OBSERVATIONS

3.1. *Luminosity Functions*

Figures 1 and 2 show the X-ray luminosity function for clusters of galaxies in the two models considered: SCDM and LCDM. Figure 1, for the SCDM model, breaks the total luminosity into standard spectral bands and compares our previous results based on bremsstrahlung emission from a (H, He) plasma (*filled squares*) to the full (line and continuum) emission (*open circles*) from a CLOUDY (Ferland 1994) mixture of elements. Two points are to be noted. First, for high-luminosity clusters ($L_x \geq 10^{44}$ ergs s^{-1}) the differences are minimal, becoming significant ($\geq$ factor of 3) only at the lowest luminosities ($L_x \approx 10^{41}$ ergs s^{-1}), where our observational knowledge is poor. This is simply a manifestation of the temperature-luminosity relation noted in both observations (Edge et al. 1990; Henry & Arnaud 1991; Henry 1992) and in the numerical simulations (Cen & Ostriker 1994). At lower luminosities the clusters have lower temperatures, leaving the atoms less fully ionized and more capable of line emission. Second, the differences are least in the hard bands such as the 1–10 keV range (Fig. 1*d*) and most in the bands shown in Figures 1*b* and 1*c*, which reach below 1 keV, where the principal line emission occurs.

Figure 2 shows the same simulated data, from the LCDM model, and shows the same differences between continuum-only and line-plus-continuum computations. The increase due to line emission is greater for the LCDM than for the SCDM model since the LCDM clusters are cooler. Overall, our prior conclusions that the SCDM model overpredicts the number of bright X-ray clusters but the LCDM model in in rough agreement with observations remains true, as the high-luminosity clusters, where comparisons to observations are cleanest, are not much affected by line emission.

3.2. *Spectral Energy Distributions*

Figures 3 and 4 show detailed spectra for the two models broken up in a different way. All the luminosity emitted in the box from regions within 1 h^{-1} Mpc at the center of a rich cluster having L_x(bolometric) $> 10^{43}$ ergs s^{-1} is shown (*solid line*) as the mean spatial emissivity due to "X-ray clusters" in ergs cm^{-3} s^{-1} eV^{-1}. But much of the hot, emitting gas is further from cluster cores, or in poor clusters or groups, or along filaments and sheets. These regions typically have such low surface brightness that current and planned instrumentation does not detect them as distinct "sources." But they should be seen in all-sky studies and will have specific spectral and angular distribution features. The gas causing this residual emission is, of course, highly clumped, but it fills a much larger fraction of the total volume than the 1.8×10^{-4} and 6.4×10^{-5} filling factors occupied by the luminous clusters in the SCDM and LCDM models, respectively. This gas is also, of course, typically at a lower temperature than the several keV gas in the great clusters. In Figure 3 the dashed lines show the volume-averaged emissivity from this background gas. Figure 3*a* shows the spectra at a resolution which roughly corresponds to the *Advanced Satellite for Cosmology and Astrophysics* (*ASCA*) experiment (Tanaka, Inoue, & Holt 1994), with the relative displacement of curves shown as computed. Figure 3*b* shows the same information with an arbitrary shift of the vertical scale and higher resolution on the horizontal scale to allow better identification of individual lines and to indicate what future experiments may find.

We note that in both models the background hot gas dominates the emission from rich clusters below approximately 1 keV. Since our problems of spatial resolution are more severe for the smaller structures producing the background than they are for computing the properties of the great clusters, we expect that an accurate calculation might increase the cluster emissivity by perhaps a factor of 2 and the background by at least a factor of 4, leading to still greater dominance of the background gas in the range $10 < h\nu < 10^3$ eV. The ratio is larger for the LCDM model than for the SCDM model because the former has relatively lower temperatures.

The steepening of the spectrum below the 1 keV seen recently by *ASCA* (see Gendreau et al. 1994), as well as the O VII lines (also noted by *ASCA*) discussed below, is tentative but direct observational evidence that the background gas we are discussing has already been detected.

This new component of soft X-ray emitting gas is only apparent when we allow properly for line emission. For example, if in Figure 4*a*, we artificially assume zero metallicity for the background gas we reduce the luminosity in the range 10–1000 eV by a factor of 3.1. The spectral signature of the background as seen in the low-resolution spectra, Figures 3*a* and 4*a*, is the "iron bump" (actually a mixture of iron, oxygen, and nitrogen) in the region 0.5–1.0 keV.

© American Astronomical Society • Provided by the NASA Astrophysics Data System

1995ApJ...451..436C

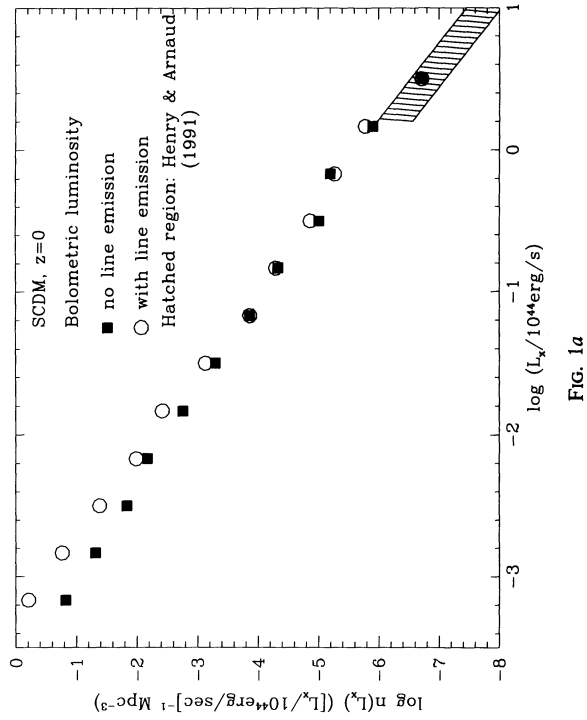

FIG. 1a

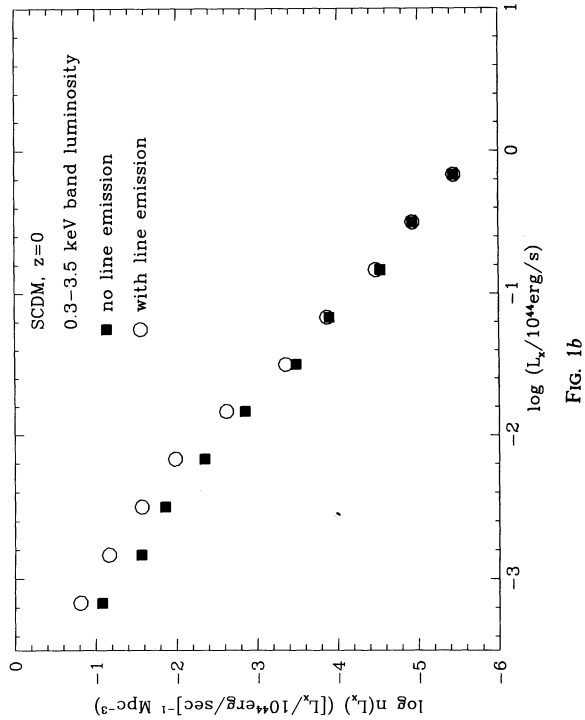

FIG. 1b

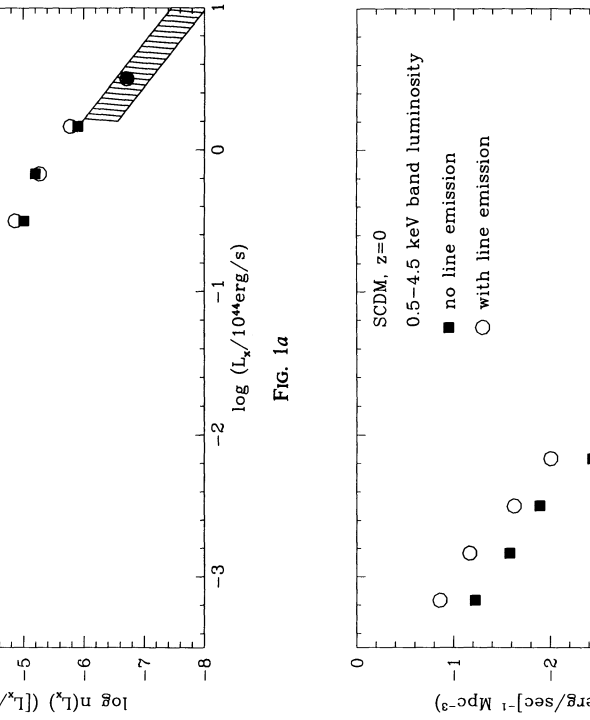

FIG. 1c

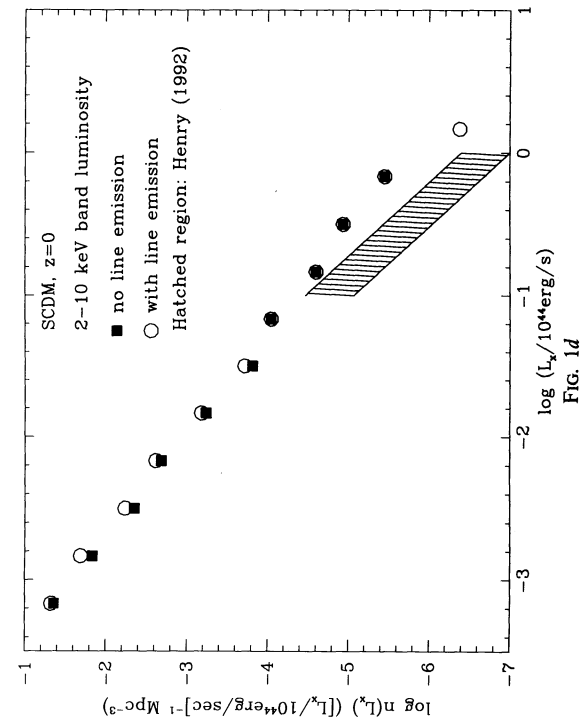

FIG. 1d

FIG. 1.—Computed luminosity functions for the SCDM model at $z = 0$, in four different bands: (*a*) bolometric, (*b*) 0.3–3.5 keV, (*c*) 0.5–4.5 keV, and (*d*) 2–10 keV. *Open circles*, Line emissions as well as bremsstrahlung; *filled squares*, only bremsstrahlung due to H and He. The hatched region in (*a*) indicates observations by Henry & Arnaud (1991), and that in (*d*) the observations of Henry (1992).

© American Astronomical Society • Provided by the NASA Astrophysics Data System

1995ApJ...451..436C

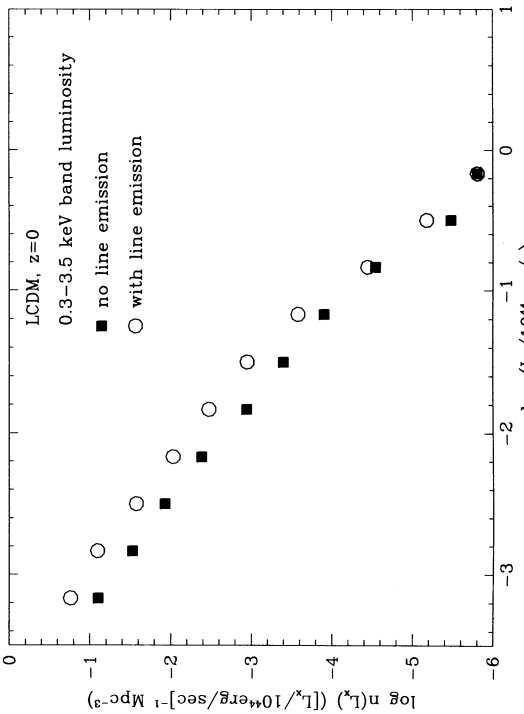

FIG. 2b

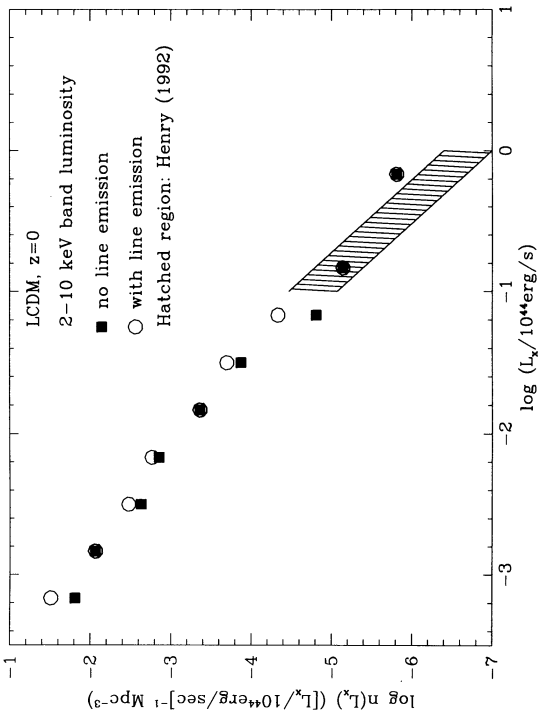

FIG. 2d

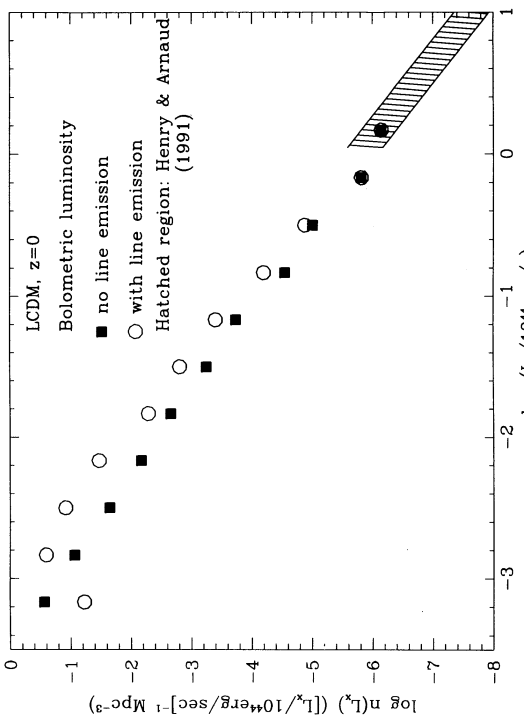

FIG. 2a

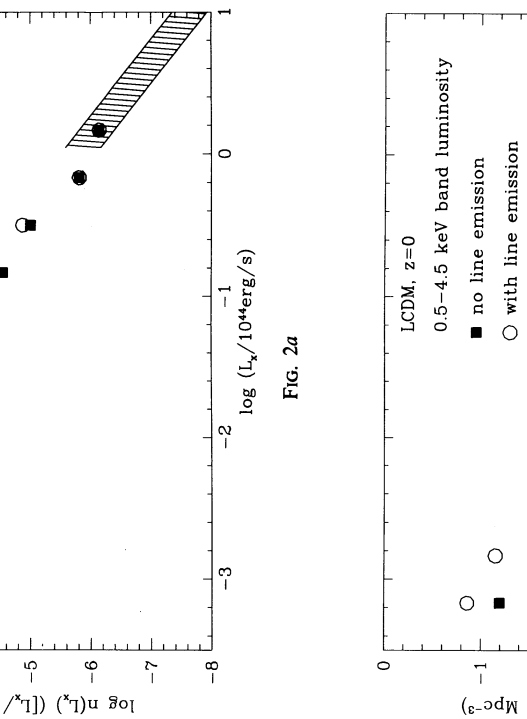

FIG. 2c

FIG. 2.—Same as Fig. 1, but for the LCDM model.

© American Astronomical Society • Provided by the NASA Astrophysics Data System

1995ApJ...451..436C

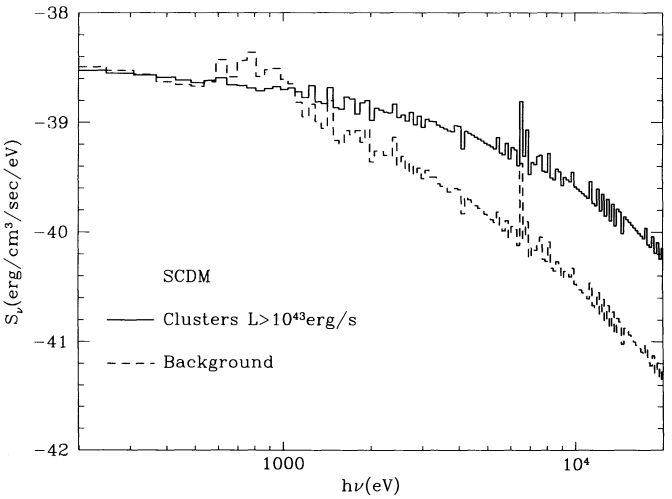

FIG. 3a

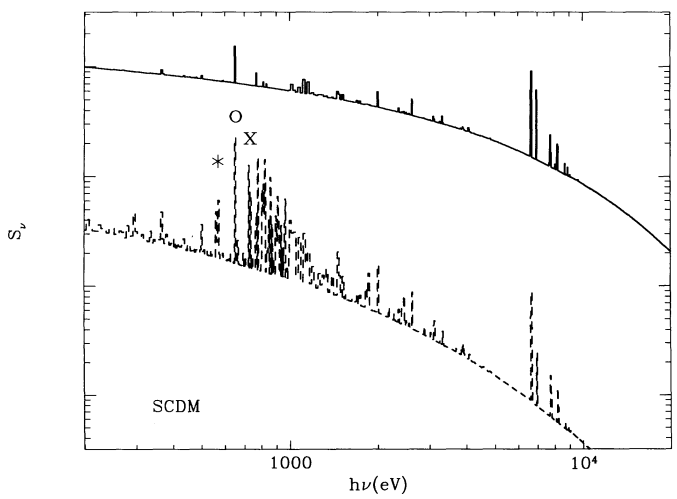

FIG. 3b

FIG. 3.—(*a*) Volume-averaged X-ray emissivity of all the bright clusters $L_{bol} > 10^{43}$ ergs s^{-1} (*solid line*) and X-ray emissivity of the background (*dashed line*) at redshift $z = 0$ for the SCDM model. We use the spectral resolution of the *ASCA* SIS detector, which has a resolution of 60 eV at 1 keV and 140 keV at 8 keV (linear interpolation is used for the range 0.4–9 keV in which the SIS detector is sensitive; below 0.4 keV we simply assume a spectral resolution of 60 eV). (*b*) High-resolution version of (*a*) with the two lines displaced vertically by an arbitrary amount for display purpose. Note the prominent "iron bump" in the background emission. We designate three temperature-sensitive lines: an O VII blend characteristic of 10^6 K gas at 0.561–0.574 keV (*asterisk*), O VIII of $10^{6.5}$ K gas at 0.654 keV (labeled "O"), and a pair of Fe XVII lines at 0.726 and 0.739 keV from gas at $10^{6.5}$ K (labeled "X").

Now let us turn to Figures 3*b* and 4*b*, which show detailed spectra that allow us to identify better those spectral lines contributing most to the background. We see in the background gas a strong signature in the region 0.561–0.574 keV (*asterisk*) from a blend of O VII lines (characteristic of 10^6 K gas) that is weak or absent in the cluster emission spectra. Also strong in the background gas is the 0.904–0.922 keV blend of lines from Ne IX at a similar temperature. Both features are nearly absent in the cluster gas. The strong O VIII line at 0.654 keV (labeled "O") seen in both cluster and background gas will give a separate indication of oxygen abundance allowing the ratio of the 0.57 to 0.65 keV features to be used as a temperature indicator. We have found one other spectral feature, which is prominent in the background gas but absent from the cluster spectra. This is a pair of Fe XVII lines at 0.726 and 0.739 keV (labeled "X") which have peak strength in gas at approximately $10^{6.5}$ K. These are strong in the background (Figs. 3*b* and 4*b*, *dashed lines*) but are not apparent in the cluster gas, where all the strong Fe lines are from higher ionization species, typically Fe XIX → Fe XXII.

Figure 5 shows typical spectra (from the LCDM model) for a high-temperature (2.7 keV), high-luminosity (1.6×10^{44} ergs s^{-1}) cluster and a lower temperature (1.8 keV), lower luminosity (3.5×10^{43} ergs s^{-1}) cluster. Overall, line emission is stronger in the lower temperature cluster, particularly the ~1 keV iron blend and the 0.654 keV O VIII line.

How can the background gas that we are discussing be distinguished from the hot Galactic gas along the same line of sight? To some extent the soft X-ray "background" that we are proposing is the same as Galactic emission in that the sum over all galaxies like our own does make a nontrivial contribution to the soft X-ray background. If the average galaxy emits 2×10^{39} ergs s^{-1} in the 0.5–1.5 keV band (see Fabbiano 1989),

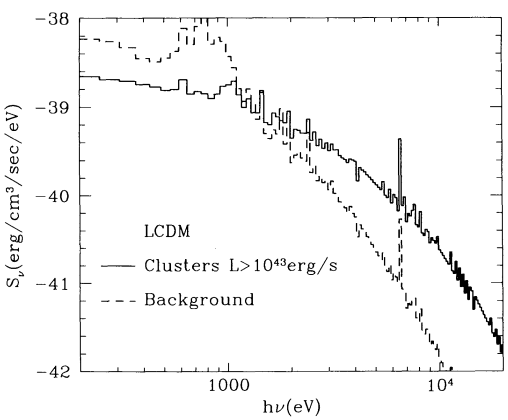

FIG. 4a

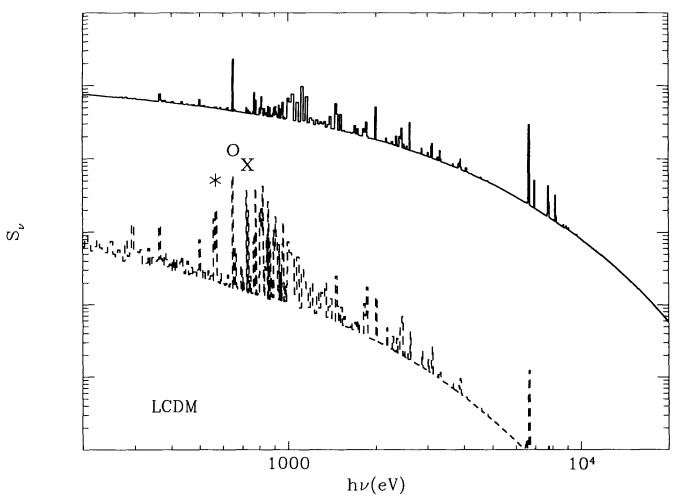

FIG. 4b

FIG. 4.—Same as Fig. 3, but for the LCDM model. Note how the background emissivity dominates the radiation from clusters below 1 keV.

© American Astronomical Society • Provided by the NASA Astrophysics Data System

1995ApJ...451..436C

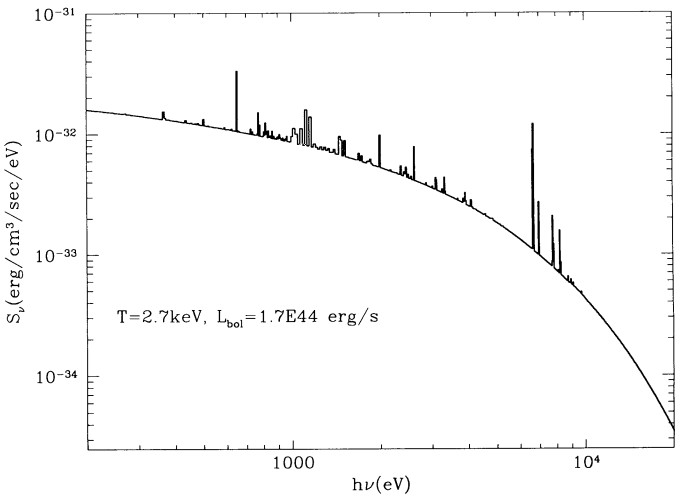

FIG. 5a

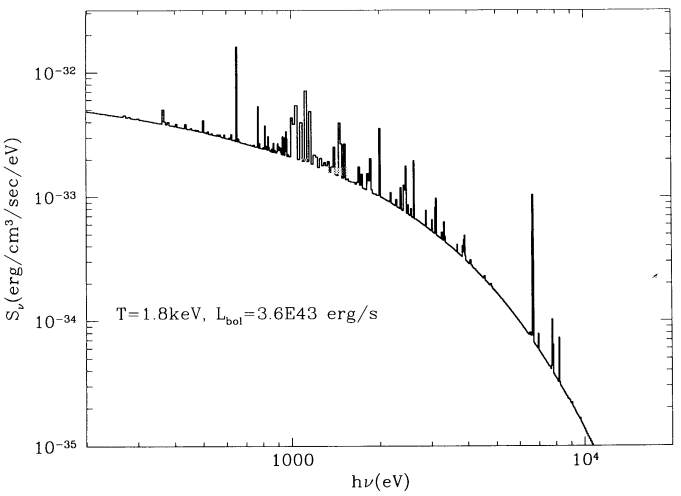

FIG. 5b

FIG. 5.—Spectra of two bright X-ray clusters for the LCDM model: (*a*) high temperature, high luminosity; (*b*) lower temperature, lower luminosity.

then the sum of all such will produce an emissivity of 10^{-39} ergs cm^{-3} s^{-1} eV^{-1}, not far from the levels shown in Figure 4*a*. But most of the emission shown by the dashed line in Figure 4*a* is due to hot gas in bigger systems than our own Galactic disk or halo. Thus, the temperature is in the range 10^6–10^7 K, whereas, for most of the Galactic coronal gas, the typical temperature (as weighted by ρ^2) is in the range 10^5–10^6 K. Thus, the line ratios indicative of the O VI/O VII and O VII/O VIII ratios will help in distinguishing between the two components. The mean logarithmic slope of S_ν will also provide an important discriminant, in that the background emission shows a much steeper slope than the cluster emission below 1 keV.

But both the line ratios and the slope of the continuum will be affected by the convolution over redshift; i.e., we see along any line of sight radiation emitted at a variety of epochs shifted by various amounts. However, this effect, which will blur out line features, is not as large as might be expected. Examination of Figure 14 of Cen & Ostriker (1944) shows that in even the softer (0.3–3.5 keV) band half of intensity arises from redshifts $z > 0.32$. Thus, the mean redshift of the emitted $\sim$1 keV photons will be close to $z = 0.32$ with a dispersion of perhaps $\sigma = 0.32$. As a consequence, the blurring of spectral features in the background will be approximately 0.32/1.3 = 24% with a shift of 32%. Specifically the iron blend should move from the region 0.6–1.0 keV (FWHM) to the region 0.45–0.81 keV with a width only slightly larger than shown in Figure 4*a*.

In fact, a strong soft X-ray background radiation field has been detected (see McCammon & Sanders 1990), but for a variety of reasons, the very low energy part of this is believed to be of Galactic rather than extragalactic origin. For example, in the C band, 0.2–0.3 keV, the minimal shadowing of the soft X-ray background by the SMC (recently reviewed by McCammon & Sanders 1990) seriously limits the extragalactic component, showing that a large fraction originates from a hot component of the interstellar medium (ISM) (see McKee & Ostriker 1977), or a hot Galactic halo. But there are reasons to believe that a significant fraction of at least the component in the range 0.5–1.0 keV is truly extragalactic (see Burrows & Kraft 1993; Gendreau et al. 1994). The spectral features which we noted earlier should help provide clues to the origin of the background radiation in this range as the Galactic component is probably too cool to produce the iron blend which should be prominent in the background component described in this paper.

3.3. *Cooling Cluster Cores*

Now let us turn to the question of cooling flows. There is abundant evidence (Fabian 1994) that in the central regions of many clusters substantial amounts of gas exist that have cooling times which are short compared to the Hubble time. We have not addressed this issue in the past for two reasons: first, since we did not include metal line emission, our cooling functions were inaccurate in just those regions where cooling might be most important; second, our spatial resolution was inadequate to examine accurately the dense central regions which are most likely to cool. We can address the first of these issues now, but our resolution, while improved over our earlier calculations, is still not sufficient to address the problem accurately so our remarks must be confined to comparative issues. For which models and which luminosity ranges is cooling of greatest importance? Figures 6 and 7 show the ratio of the Hubble time to the cooling time for the central cell in each cluster, Figure 6 showing the distributions of this ratio for the SCDM model and Figure 7 the distributions for the LCDM model. The volume of the central cell is (315 h^{-1} kpc)^3 which corresponds to a sphere of radius 195 h^{-1} kpc. Given the unavoidable numerical diffusion, a more accurate estimate of our effective central cell radius might be approximately 250 h^{-1} kpc. In both Figures 6 and 7 we divide the clusters into three groups based on the total bolometric luminosity. We see that for the highest luminosity clusters ($L_{bol} > 10^{43}$ ergs s^{-1}) the computed cooling times are very long on average compared to the Hubble time. For the SCDM model t_H/t_{cool} is always less than 0.03, and for the LCDM model it is less than 0.06. However, our computed sample size is small, and it seems likely that the tail would reach a value of t_H/t_{cool} which is a factor of 10 higher were the sample size to include 100 bright clusters. This issue of a small statistical sample plus our relatively poor resolution make it likely that perhaps a few percent of the bright clusters would have cooling cores in perfect simu-

© American Astronomical Society • Provided by the NASA Astrophysics Data System

1995ApJ...451..436C

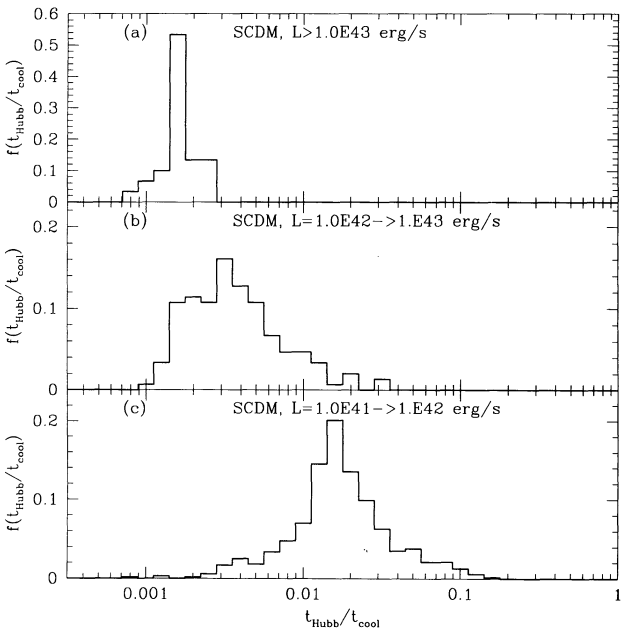

FIG. 6.—Histograms of the ratio t_H/t_{cool} for X-ray clusters in three different luminosity bands, for the SCDM model.

lations of these two models. Work currently in progress should greatly clarify this issue.

But we can say with some certainty that the lower luminosity clusters, since they have lower temperatures, cool much more efficiently. This is especially evident in the LCDM model (Fig. 7*c*), where it is clear that cooling would be an important effect for higher resolution simulations.

The trend for the increased importance of cooling in Figures 6 and 7 as we go from panels (*a*) to (*c*) is evident (low-luminosity regions are more subject to cooling than high-luminosity regions) and strengthens the conclusions of § 3.1.

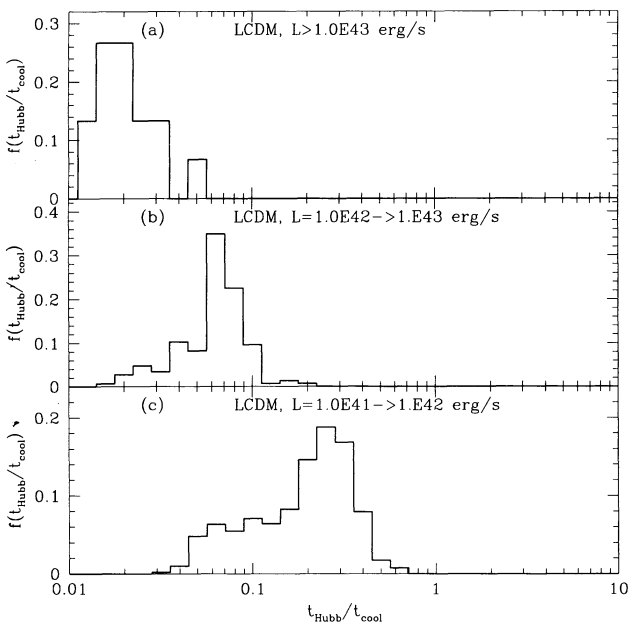

FIG. 7.—Same as Fig. 6, but for the LCDM model. Cooling should be important in low-luminosity clusters.

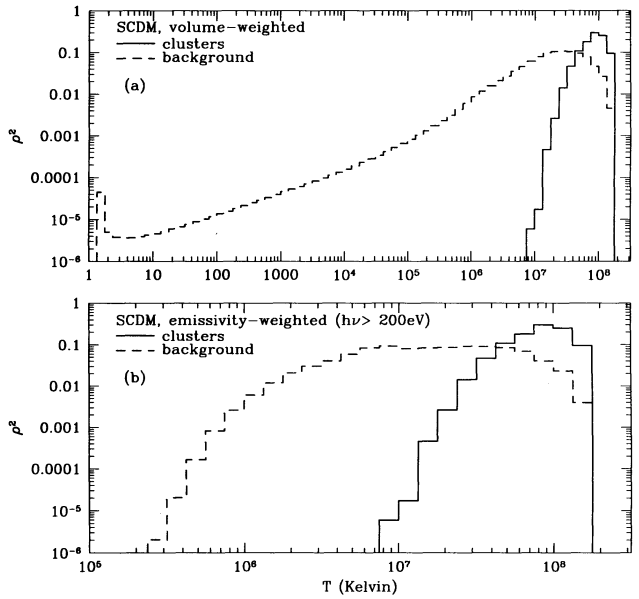

FIG. 8.—Plot of ρ^2 for the SCDM model at $z = 0$, on the cell scale as a function of temperature in two different ways: (*a*) volume weighted and (*b*) emissivity weighted ($\int_{200eV}^{10keV} S_\nu\, d\nu$). Each panel is further broken into two different components: clusters and background. Note that the background radiation is emitted by considerably lower temperature gas than that producing the cluster emission.

When cosmic gas cools, it typically contrasts to a higher density and thus cools still more rapidly. Thus, if we had allowed for cooling in the evolution of the gas, then the background emission that we found would have been still stronger with respect to the average cluster emission.

4. CONCLUSIONS

Straightforward physical theory predicts that the gravitationally induced growth of structure will lead to an accumulation of hot shocked gas at the vertices where caustics intersect.

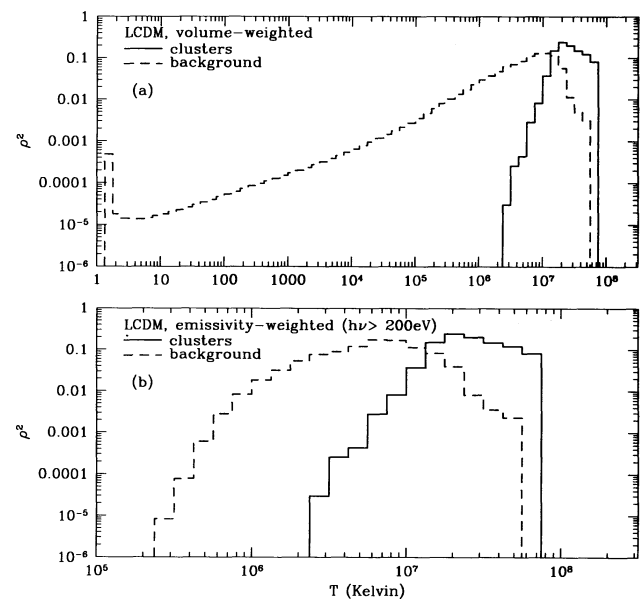

FIG. 9.—Same as Fig. 8, but for the LCDM model.

© American Astronomical Society • Provided by the NASA Astrophysics Data System

1995ApJ...451..436C

Numerical simulations have in fact confirmed that some models for the growth of cosmological structure do fit rather nicely the X-ray observations of clusters of galaxies. However, the same theories also predict the existence of much more hot gas, at a somewhat lower temperature, filling a significant fraction of cosmic space with X-ray–emitting sheets and filaments. In this paper we compute the spectral properties of this "background" gas, noting that it should dominate over the cluster gas (in total emissivity) at energies below 1 keV.

Figure 8 for SCDM and Figure 9 for LCDM summarize the nature of the regions emitting the two components at redshift zero, Figures 8*a* and 9*a* showing the volume-weighted distribution of ρ^2 (as a function of gas temperature) and Figures 8*b* and 9*b* the emissivity-weighted ($\int_{200\,\mathrm{eV}}^{10\,\mathrm{keV}} S_\nu\, d\nu$) distribution. Examining Figure 9*b* we see that the cluster X-rays are typically emitted from gas in the range $10^{7.0-7.8}$ K whereas the background gas emission is broadly distributed in the range $10^{6.0-7.3}$ K. The signature of the background gas will be a softer spectrum, certain specific lines and blends, and a spatial extent which is much more diffuse (in terms of the angular autocorrelation function) than the cluster gas. The long-standing problem that the spectrum of the background does not match well to the spectrum of the resolved sources remains with us. Further, as pointed out by Hasinger et al. (1993) and earlier by Hamilton & Helfand (1987), there is room, even perhaps the necessity for either a very faint unclustered population of sources or a more smoothly distributed component. Also, recent *ASCA* measurements (Gendreau et al. 1994) indicate the existence of a background component with a steep spectrum below 1 keV and evidence from O VII lines. Thus it may be that *ROSAT*, *ASCA*, and other satellites have already observed the emission from this background gas, but because of the diffuse nature of the gas, rather specific analyses of the observational data must be undertaken to confirm the detection.

We are happy to acknowledge support from grants NAGW-2448 and AST91-08103. It is a pleasure to acknowledge NCSA for allowing us to use their Convex-3880 supercomputer. We are extremely grateful to John C. Raymond who generously provided the computer code that enabled us to compute line and continuum emission rates for heavy elements. Discussions with H. Bohringer, B. Draine, G. Hasinger, R. Mushotzky, B. Paczynski, A. Soltan, and J. Trümper are gratefully acknowledged.

REFERENCES

Arnaud, K., et al. 1994, preprint
Arnaud, M., Rothenflug, R., Boulade, O., Vigroux, L., & Vangloni-Flam, E. 1992, A&A, 254, 49
Bryan, G. L., Cen, R., Norman, M. L., Ostriker, J. P., & Stone, J. M. 1994, ApJ, 428, 405
Burrows, D. N., & Kraft, R. P. 1993, ApJ, 411, 685
Cen, R., & Ostriker, J. P. 1994, ApJ, 429, 4
Cen, R., Ostriker, J. P., Soltan, A. M., & Hasinger, G. 1995, in preparation
Cowie, L. L., Songaila, A., Kim, T. S., & Hu, E. 1995, AJ, in press
Edge, A. C., & Stewart, G. C. 1991, MNRAS, 252, 428
Edge, A. C., Stewart, G. C., Fabian, A. C., & Arnaud, K. A. 1990, MNRAS, 245, 559
Fabbiano, G. 1989, ARA&A, 27, 89
Fabian, A. C. 1994, ARA&A, 32, 277
Fan, X.-M., & Tytler, D. 1994, ApJS, 97, 17
Ferland, G. J. 1994, preprint
Gendreau, K. C., et al. 1994, preprint
Hamilton, T. T., & Helfand, D. J. 1987, ApJ, 318, 93
Hasinger, G., Burg, R., Giacconi, R., Hartner, G., Schmidt, M., Trumper, J., & Zamorani, G. 1993, A&A, 275, 1
Henry, J. P. 1992, in Clusters and Superclusters of Galaxies, ed. A. C. Fabian (Dordrecht: Kluwer), 311
Henry, J. P., & Arnaud, K. A. 1991, ApJ, 372, 410
Kang, H., Cen, R., Ostriker, J. P., & Ryu, D. 1994, ApJ, 428, 1
McCammon, D., & Sanders, W. T. 1990, ARA&A, 28, 657
McKee, C. F., & Ostriker, J. P. 1977, ApJ, 218, 148
Raymond, J. C., & Smith, B. W. 1977, ApJS, 35, 419
Soltan, A., Hasinger, G., Bohringer, H., & Trumper, J. 1995, preprint
Tanaka, Y., Inoue, H., & Holt, S. S. 1994, PASJ, 46, L37

© American Astronomical Society • Provided by the NASA Astrophysics Data System